Available online at www.sciencedirect.com
ScienceDirect
Journal of Photochemistry and Photobiology A: Chemistry 195 (2008) 314–322
Journal of Photochemistry and Photobiology A:Chemistry
www.elsevier.com/locate/jphotochem

Two photoactive lanthanide (Eu^{3+}, Tb^{3+}) hybrid materials of modified β-diketone bridge directly covalently bonded mesoporous host (MCM-41)

Bing Yan [a,b,*], Bing Zhou [a]

[a] *Department of Chemistry, Tongji University, Shanghai 200092, China*
[b] *State Key Lab of Rare Earth Materials Chemistry and Applications, Peking University, Beijing 100871, China*

Received 17 May 2007; received in revised form 24 October 2007; accepted 29 October 2007
Available online 4 November 2007

Abstract

In this context, two β-diketone ligands, dibenzoylmethane (DBM) and acetylacetone (ACAC) were modified with 3-(triethylsilyl)-propyl-isocyanate (TEPIC) through the extraction of hydrogen of ethylene groups. Then Eu^{3+} and Tb^{3+} complexes with the two modified ligands (DBM-Si and ACAC-Si) were fabricated to mesoporous host (MCM-41) by template-directed co-condensation of tetraethyl orthosilicate, resulting in two kinds of novel covalently bonded hybrid materials (denoted as DBM-MCM-41 and ACAC-MCM-41). XRD, N_2 adsorption/desorption and SEM reveal that the two covalently bonded hybrid materials have high surface area, uniform mesopore structure and good crystallinity. Especially the luminescent properties present that the modified dibenzoylmethane (DBM-Si) could sensitize Eu(III) ions to exhibit red luminescence and the modified acetylacetone (ACAC-Si) could sensitize Tb(III) ions to exhibit green luminescence, respectively. The hybrid materials covalently bonded MCM-41 possess the higher intensities and longer lifetimes than those of pure complexes (Eu-DBM and Tb-ACAC).

Keywords: Photophysical properties; Sol–gel process; Molecular hybrids; Modified β-diketone bridges directly covalently bonded mesoporous host

1. Introduction

The discovery of periodic, ordered mesoporous molecular sieves M41s [1,2] received considerable attention due to their high specific surface area (700–1500 $m^2\,g^{-1}$) as well as their uniform pore size (varying from 1.5 to 10 nm), which can favor them new functions and applications [3]. There have been many reports on the modification of inorganic mesoporous materials such as MCM-41 silica via post-grafting [4,5] or via direct routes involving the co-condensation of tetraalkoxysilanes and organo-functionalized tri-alkoxysilanes [6–10], which is also referred to as one-pot synthesis. The latter approach for synthesis of MCM-41 has been the preferred route for most researchers because of the easier one-pot synthetic protocol and better control of organosilane loading and distribution [11–13]. Besides the advantages of high surface area, large pore volume and outstanding thermal stabilities, there are a large number of hydroxyl in MCM-41, which provide necessary qualification for the modification of inner face and self assembly of huge guest molecules, namely, providing outstanding hosts for self aggregation chemistry. Many research efforts are focused on preparing the organic/inorganic hybrids through the functionalization of the exterior and/or interior surfaces, prompting the utilization of MCM-41 in many fields.

Lanthanide-containing hybrid materials have stimulated great research interest for their excellent luminescent properties [14] and the special functions make them widely applied in various fields such as photonic crystal [15,16], optical glasses [17] and fluorescent or laser systems [18]. Generally speaking, inorganic matrices doped with a metal complex, especially with lanthanide organic complexes have already been found to show superior emission intensities, and organic components are considered to be efficient sensitizers for the luminescence of rare earth ions (so-called "antenna effect") [19–25]. However, such doped strategy cannot solve the problem of quenching effect of luminescent centers because the high energy vibration brought by the surrounding hydroxyl groups and weak interactions (such as hydrogen bonding, van der Waals force or electrostatic forces) mainly functionalize between organic and inorganic components

* Corresponding author at: Department of Chemistry, Tongji University, Shanghai 200092, China. Tel.: +86 21 65984663; fax: +86 21 65982287.
E-mail address: byan@tongji.edu.cn (B. Yan).

1010-6030/$ – see front matter © 2007 Elsevier B.V. All rights reserved.
doi:10.1016/j.jphotochem.2007.10.019

[26]. Moreover, inhomogeneous dispersion of two phases and leaching of the photoactive molecules often occur in this sort of hybrid materials for which the concentration of complex is also greatly reduced. As a result, a few studies in term of covalently bonded hybrids with increasing chemical stability have appeared and the as-derived molecular-based materials exhibit monophasic appearance even at a high concentration of lanthanide complexes [27,28]. Our research team recently put more emphasis on rare earth coordination behavior and we have now developed modified aromatic acids as 'molecular bridge' which not only can develop chelating effects that can bind to rare earth ions, but also anchor a silica matrix with an alkoxysilane group [29–32]. Besides, the modification of β-diketones and rare earth β-diketones chelates directly covalently bonded silica host have not been reported in spite of their strong luminescence for β-diketones ligands are not easy to be modified. Several reports are available on the covalent grafting of rare earth beta-diketones chelates to silica host while these hybrids were fabricated with ternary rare earth complexes systems, which belongs to other ligands such as 1,10-phenanthroline (not beta-diketones) bridge covalently bonded hybrids while beta-diketones only behave as a second ligand to Ln^{3+} [33–37]. In place of simple inorganic host precursor of TEOS, mesoporous host such as MCM-41 can also be used as host to form the covalently bonded hybrids, both of the these hybrids were bridged to mesoporous host by 1,10-phenanthroline derivatives, and 2-thenoyltrifluoroacetone is only for the second ligands to rare earth ions [33–35].

In this context, we have first prepared the MCM-41 host via a co-condensation method based on ammonia-catalyzed reactions of tetraethoxysilane (TEOS) in the presence of a low concentration of cetyltrimethylammoniumbromide (CTAB) surfactant. Then we attempt to modify active methylene of DBM and ACAC by TESPIC bearing tri-alkoxysilyl group as two functionalized organic ligands (DBM-Si and ACAC-Si) under sufficient basic environment. Subsequently, we use the two novel ligands as molecular bridge to connect MCM-41 through the hydrolysis and polycondensation reactions among triethoxysilyl of DBM-Si (or ACAC-Si) and the Si–OH of MCM-41 as well as to coordinate to lanthanide ions through carbonyl groups.

2. Experimental

2.1. Preparation of DBM-Si and ACAC-Si monomer

3-(Triethylsilyl)-propyl-isocyanate (TEPIC) was purchased from Lancaster Synthesis Ltd. The solvents used were purified by common methods. Other starting reagents were used as received. A typical procedure for the preparation of DBM-Si was as follows: 2 mmol dibenzoylmethane was first dissolved in refluxing dehydrate tetrahydrofuran (THF) by stirring and 4 mmol NaH (0.16 g, 60%) was added to the solution. Two hours later, 4 mmol (1.0 g) 3-(triethoxysilyl)-propyl-isocyanate was then put into the solution by drops for half an hour. The whole mixture was refluxing at 60 °C under argon for 12 h. After isolation and purification, a yellow oil DBM-Si was furnished. IR: –CONH– 1693 cm^{-1}, $-(CH_2)_3-$ 2925 cm^{-1}, Si–O 1090 cm^{-1}. ^1H NMR ($CDCl_3$) $C_{35}H_{54}O_{10}N_2Si_2$: δ 8.05(2H, t), 7.58(4H, m), 7.18(2H, s), 6.91(2H, s), 6.60(2H, brs), 3.82(12H, m CH_2(OEt)), 3.62(2H, brs), 3.16(2H, m), 1.86(6H, m), 1.61(2H, m), 1.22(14H, m, CH_3(OEt)), 0.63(4H, t). The ACAC-Si monomer was prepared similarly. ^1H NMR ($CDCl_3$, 500 MHz) $C_{25}H_{50}O_{10}N_2Si_2$: δ 8.03(2H, bs, NH), 3.83(12H, q, CH_2(OEt)), 3.52(4H, t), 2.23(6H, s, CH_3), 1.82(4H, m), 1.23(18H, t, CH_3(OEt)), 0.72(4H, t).

2.2. Preparation of the MCM-41 mesoporous host

The MCM-41 host structure was prepared as Ref. [36]: in a typical synthesis procedure, cetyltrimethylammoniumbromide (5 g) were first dissolved in 200 g of deionized water under heating at 60 °C until a clear aqueous solution was obtained. To this solution were added 55 mL of NH_3. H_2O and 23 mL of tetraethyl orthosilicate (TEOS), bringing the pH value up to about 11.6. After stirring for 3 h, the solution was placed in a Teflon-lined vessel and heated at 110 °C for 120 h. The resulting white powder was filtered, thoroughly washed with deionized water and dried at room temperature. The CTAB surfactant molecules were then removed by calcination of the resulting white powder at 600 °C in air for 6 h. The resulting product is afterwards designated as calcined MCM-41.

2.3. Modification of MCM-41 by DBM-Si and ACAC-Si and the preparation of the two covalently bonded hybrid materials with mesoporous host

A controlled amount of DBM-Si (2.155 g, 3.0 mmol) was first dissolved in a minimum amount of *N*,*N*-dimethylformamide (5 mL) with stirring and 20 mL ethanol was added in it for dilution. Then appropriate amount of MCM-41 (molar ratio of MCM-41:DBM-Si:60: (1) were added to the solution. Six hours latter, corresponding amount of $Eu(NO_3)_3{\cdot}6H_2O$ (0.446 g, 1.0 mmol) was added and stirred vigorously in air at room temperature for 48 h. Finally, the solid product is recovered by centrifugation, washed with ethanol, dried at 80 °C for 4 h and finally as a powder in a desiccator (see Fig. 1). This covalently bonded hybrid material with mesoporous host containing Eu^{3+} ions was denoted as Eu-DBM-MCM-41. Using similar method, DBM-Si and $Eu(NO_3)_3{\cdot}6H_2O$ were taken place by ACAC-Si (1.782 g, 3.0 mmol) and $Eu(NO_3)_3{\cdot}6H_2O$ (0.453 g, 1.0 mmol), respectively. Then another covalently bonded hybrids with mesoporous host containing Tb^{3+} ions was prepared (denoted as Tb-ACAC-MCM-41).

2.4. Physical measurements

All measurements were completed under room temperature except that phosphorescence spectra (5×10^{-4} mol dm^{-3} acetone solution) were measured under 77 K. ^1H NMR spectra were recorded in $CDCl_3$ on a Bruker AVANCE-500 spectrometer with tetramethylsilane (TMS) as internal reference. Ultraviolet absorption spectra of these powder samples (5×10^{-4} mol dm^{-1} acetone solution) were recorded with an Agilent 8453 spectrophotometer. Photoluminescent excitation and emission spectra were obtained on a PerkinElmer LS-

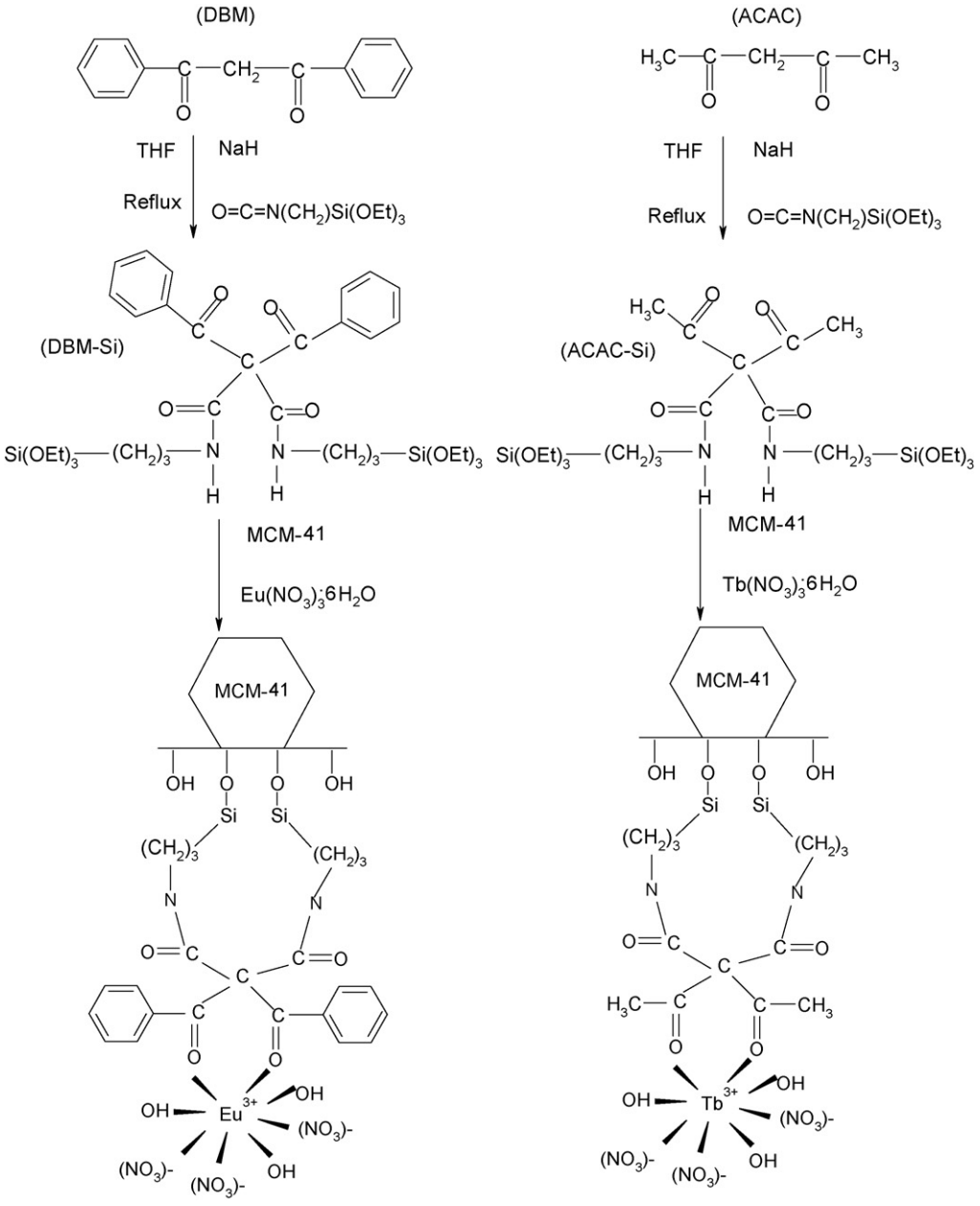

Fig. 1. Predicted structure of covalently bonded hybrid materials with mesoporous structure.

55 spectrophotometer: excitation slit width = 10 nm, emission slit width = 5 nm. In order to compare the relative intensities significantly, all the experimental conditions (optical set-up, focalization point and illuminated cross-section, sample holder and emission and excitation slits width) were remained constant. Powder X-ray diffraction patterns were recorded on a Rigaku D/max-rB diffractometer equipped with a Cu anode in a 2θ range from 0.6° to 5.994°. Surface areas/total pore volumes and pore size distributions were extracted from these isotherms using the BET and BJH methods, respectively. For nitrogen sorption isotherms, about 0.10 g sample was weighted into a Pyrex sample tube and evacuated to 80 mTorr overnight at RT and then backfilled with He. The amount of nitrogen adsorbed or desorbed at liquid-nitrogen temperature as a function of pressure was measured with static physicalsorption experiments. The microstructures were checked by scanning electron microscope (SEM, Philips XL-30).

3. Results and discussion

The IR spectra of DBM (A), and DBM-Si (B) were given in the panel (I) of Fig. 2. From A to B, we could observe that the vibration of –CH_2– at 3060 cm^{-1} (A) was taken place by a strong broad band located at around 2921 cm^{-1} (B) which designated the three methylene groups of 3-(triethoxysilyl)-propyl isocyanate. Furthermore, the bands centered at 3386 cm^{-1} correspond to the stretching vibration of grafted –NH groups. In addition, the peaks at 1562 and 1509 cm^{-1} were ascribed to the bending vibration of N–H groups corresponding to the "amide II" mode. Several new peaks at 1778 and 1704 cm^{-1} are due

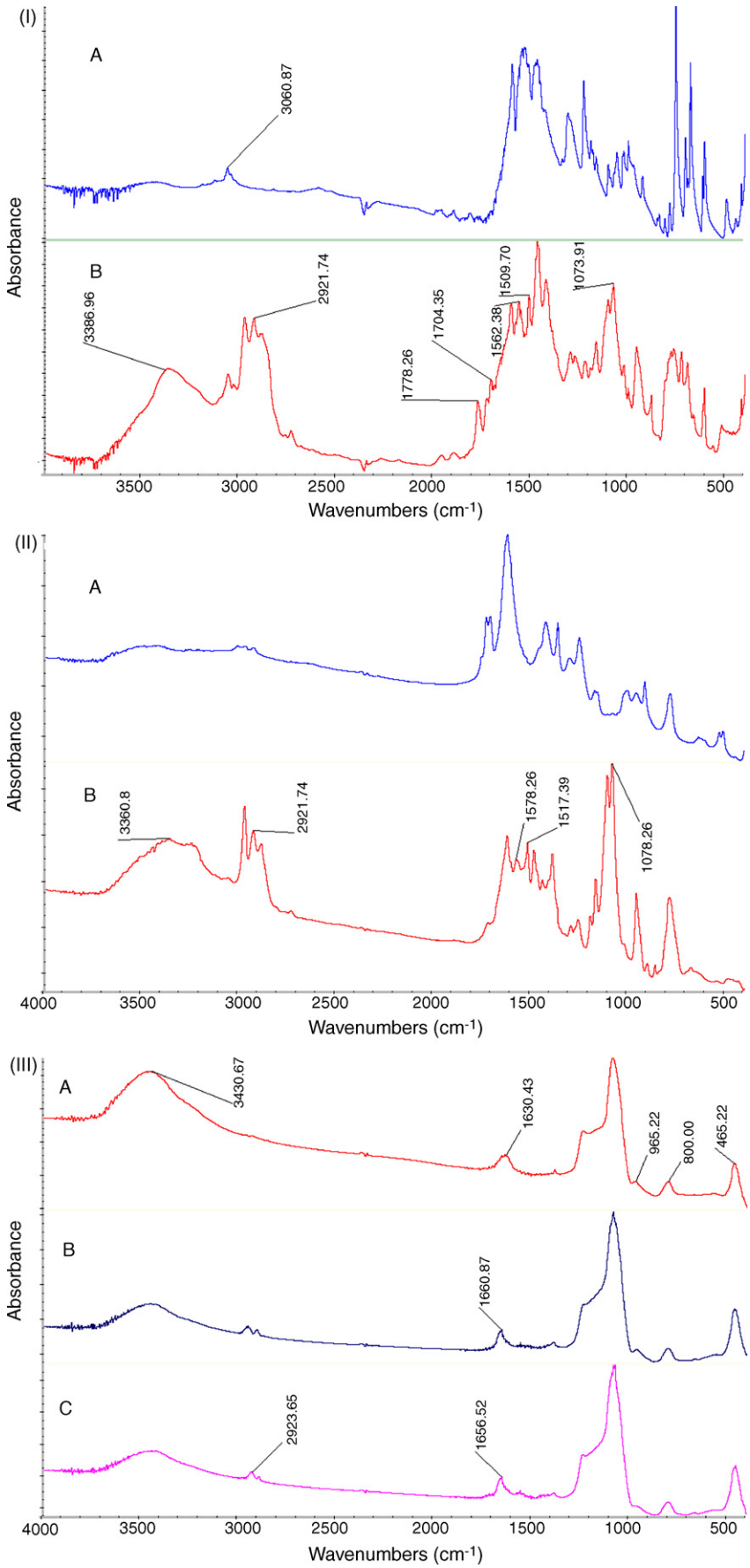

Fig. 2. The IR spectra: (I) DBM (A), and DBM-Si (B); (II) ACAC (A), and ACAC-Si (B); (III) MCM-41 (A), the Eu-DBM-MCM-41 (B) and the Tb-ACAC-MCM-41 (C).

to the C=O absorptions of TESPIC, indicating that hydrogen bonded C=O groups were largely connected with each other in terms of Carlos's research [37] about the grafted "amide I" mode. The IR spectra of ACAC (A), and ACAC-Si (B) were given in the panel (II) of Fig. 2. From A to B, we could also observe that a new strong broad band located at around 2921 cm^{-1} (B) appeared which designated the three methylene groups of 3-(triethoxysilyl)-propyl isocyanate. Furthermore, the bands centered at 3360 cm^{-1} correspond to the stretching vibration of grafted –NH groups. In addition, a new peak at 1578 cm^{-1} was ascribed to the bending vibration of N–H groups. In conclusion, TESPIC was successfully grafted onto the CH_2 groups of the coupling agent. The IR spectra of MCM-41 (A), the Eu-DBM-MCM-41 (B) and the Tb-ACAC-MCM-41 (C) were shown in panel (III) of Fig. 2. The strongest absorption bands relative to the silica host structure appear in the range of 1000–1250 cm^{-1} and are due to asymmetric Si–O stretching vibration modes, whereas the peak at 800 cm^{-1} can be attributed to the symmetric Si–O stretching vibration. The Si–O–Si bending vibration can be observed at 465 cm^{-1}, and the bands at 965 cm^{-1} can be assigned to stretching vibrations of Si–OH surface groups [38,39]. In addition, the presence of hydroxyl can be clearly evidenced by the peak at 3430 cm^{-1}. The Eu-DBM-MCM-41 and the Tb-ACAC-MCM-41 show the similar infrared absorption bands as the silica framework except a broad adsorption located at around 2923 cm^{-1}, which are just the absorption bands of $-CH_2-$, indicating that DBM-Si and ACAC-Si have been grafted onto the wall of MCM-41.

The phosphorescence spectra of Gd-DBM and Gd-DBM-Si were measured owing to its high phosphorescence–fluorescence ratio compared to those of the other Ln^{3+} complexes and Gd^{3+} can sensitize the phosphorescence emission of ligands (Fig. 3A). From the shortest wavelength of the phosphorescence emission band at 492 nm corresponded to be the 0–0 transition of Gd-DBM, the lowest triplet state energy of DBM can be determined to be 20,320 cm^{-1}, which take agreement with the data from Ref. [40]. While the low temperature phosphorescence spectrum of Gd-DBM-Si show a broad band of maximum peak at 500 nm without clear splits as Gd-DBM. The triplet state energy of DBM-Si can also be estimated to be around 20,000 cm^{-1} caused by the modification with TESPIC. The same comment is applied to the ACAC and ACAC-Si emission spectrum, as shown in Fig. 3B. From the shortest wavelength of the phosphorescence emission band at 395 nm corresponded to be the 0–0 transition of Gd-ACAC, the lowest triplet state energy of ACAC can be determined to be 25,300 cm^{-1}, corresponding to the data from Ref. [40]. Compared with Gd-ACAC, the low temperature phosphorescence spectrum of Gd-ACAC-Si show a broad band of maximum peak at 401 nm and the triplet state energy of ACAC-Si can be estimated to be around 24,940 cm^{-1} for the introduction of TESPIC group. According to Sato's result and energy transfer mechanism [40–43], the energy differences between the triplet state energy of DBM-Si (or ACAC-Si) and the resonant emissive energy level of Eu^{3+} (around 17,300 cm^{-1}) (or Tb^{3+}, about 20,500 cm^{-1}) are 3020 and 4440 cm^{-1}, respectively. We can draw a conclusion that there exist good energy match between DBM-Si or ACAC-Si and Eu^{3+} or Tb^{3+} ions,

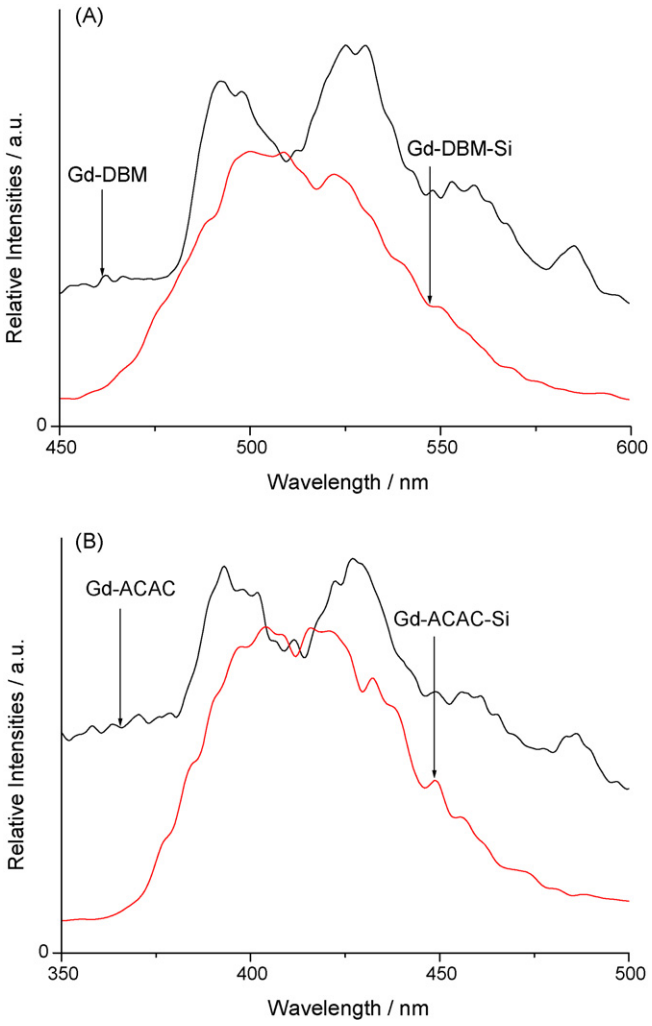

Fig. 3. The phosphorescence spectra: (I) DBM (λ_{ex} = 236 nm) (A) and DBM-Si (λ_{ex} = 237 nm) (B); (II) ACAC (λ_{ex} = 255 nm) (A) and ACAC-Si (λ_{ex} = 258 nm) (B).

and the modification of DBM and ACAC have not give rise to big change of emissive energy level of ligands. The effective luminescence for the two kinds of hybrid materials can be predicted.

Fig. 4 shows the XRD pattern of the MCM-41 host, Eu-DBM-MCM-41 and Tb-ACAC-MCM-41 characteristic of a mesostructure with a highly ordered hexagonal arrangement. Three well-defined Bragg peaks in the low angle range ($0.6° < 2\theta < 6°$) corresponded to the (1 0 0), (1 1 0), and (2 0 0) planes of the solid that are fully indexed to a hexagonal unit cell. In addition, we observe a decrease of the relative reflection intensity of d(1 0 0) XRD peak after MCM-41 was modified. So it is estimated that the modification of MCM-41 leaded to the inherent disorder and decreased the size of mesopores slightly, but not resulted in the collapse in the pore structure of covalently bonded hybrids with mesoporous host. The presence of d(1 0 0) peak suggested that the frame work stability was still maintained for Eu-DBM-MCM-41 and Tb-ACAC-MCM-41. The pore size of samples can be calculated from the X-ray diffraction interplanar spacing using the equation [44], $W_d = cd[\rho V_p/(1 + \rho V_p)]^{1/2}$, where W_d is the pore size, V_p is the primary volume (resulting

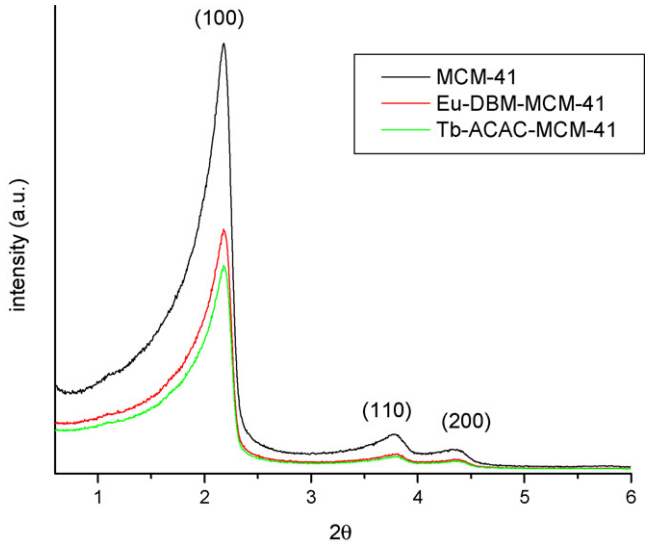

Fig. 4. The XRD pattern of the MCM-41 host, Eu-DBM-MCM-41 and Tb-ACAC-MCM-41.

Table 1
Structure and chemical data for MCM-41 host and the hybrid materials

	d_{100} (nm)	W_d (nm)	BET ($m^2\ g^{-1}$)	V ($cm^3\ g^{-1}$)	D_p (BJH, nm)
MCM-41	4.15	3.76	731.53	0.73	3.53
Eu-DBM-MCM-41	4.19	3.63	632.56	0.59	3.46
Tb-ACAC-MCM-41	4.14	3.57	605.32	0.57	3.41

from N_2 physisorption), ρ the pore wall density (ca. 2.2 $cm^3\ g^{-1}$ for siliceous materials), d the XRD(100) interplanar spacing (i.e., 37.4 for MCM-41) and c is a constant dependent on the assumed pore geometry and is equal to 1.155 for hexagonal models. The detailed data are shown in Table 1.

Fig. 5 shows the curves of the N_2 adsorption–desorption isotherms of the MCM-41 host, Eu-DBM-MCM-41 and Tb-ACAC-MCM-41. We could observed that the three isotherms were quite similar and exhibited complementary textural and framework-confined covalently bonded hybrid material with mesoporous host and uniform pore channels, as indicated by the presence of the sharp step in the $p/p_0 = 0.3$–0.37 region. Incorporation of Eu(DBM-Si)$_3$ and Tb(ACAC-Si)$_3$ into MCM-41 resulted in the reduction of the surface area from 731.53 $m^2\ g^{-1}$ for the MCM-41 to 632.56 $m^2\ g^{-1}$ for the Eu-DBM-MCM-41 and 605.32 $m^2\ g^{-1}$ for Tb-ACAC-MCM-41 (Table 1), suggesting that micro-environment of MCM-41 has moderately changed due to the introduction of luminescent centers. Likewise, the pore volume for MCM-41 for 0.73 $cm^3\ g^{-1}$ decreased to 0.59 $cm^3\ g^{-1}$ for Eu-DBM-MCM-41 and 0.57 $cm^3\ g^{-1}$ Tb-ACAC-MCM-41.

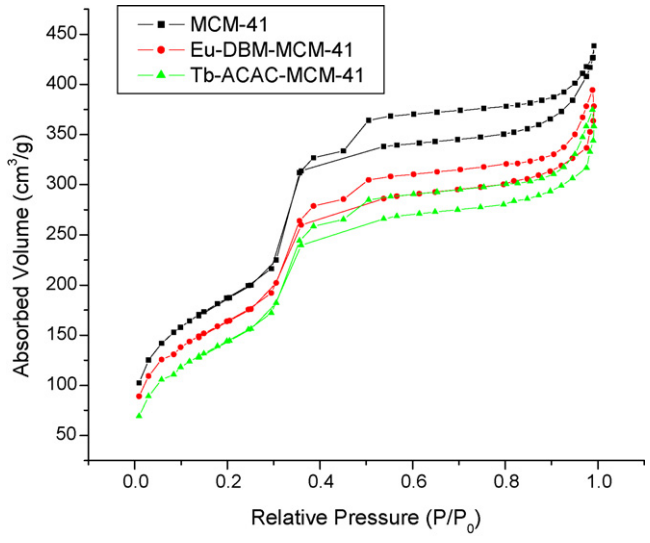

Fig. 5. The curves of the N_2 adsorption–desorption isotherms of the MCM-41 host, Eu-DBM-MCM-41 and Tb-ACAC-MCM-41.

Scanning electron microscopy (SEM) is used to determine the particle size and particle morphology of the synthesized materials. SEM pictures of the Eu-DBM-MCM-41 (A) and the Tb-ACAC-MCM-41 (B) are given in Fig. 6. And the two SEM pictures are typical for the covalently bonded hybrids with mesoporous host and show the morphology of spherical particles. It is clear that most of the particles are spherical.

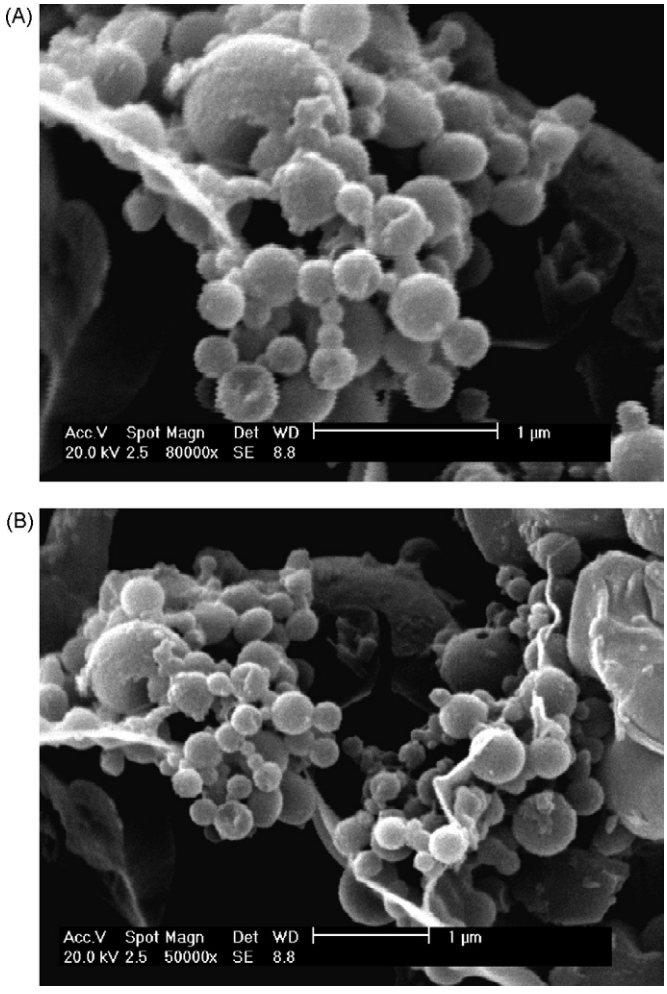

Fig. 6. SEM pictures of the Eu-DBM-MCM-41 (A) and the Tb-ACAC-MCM-41 (B).

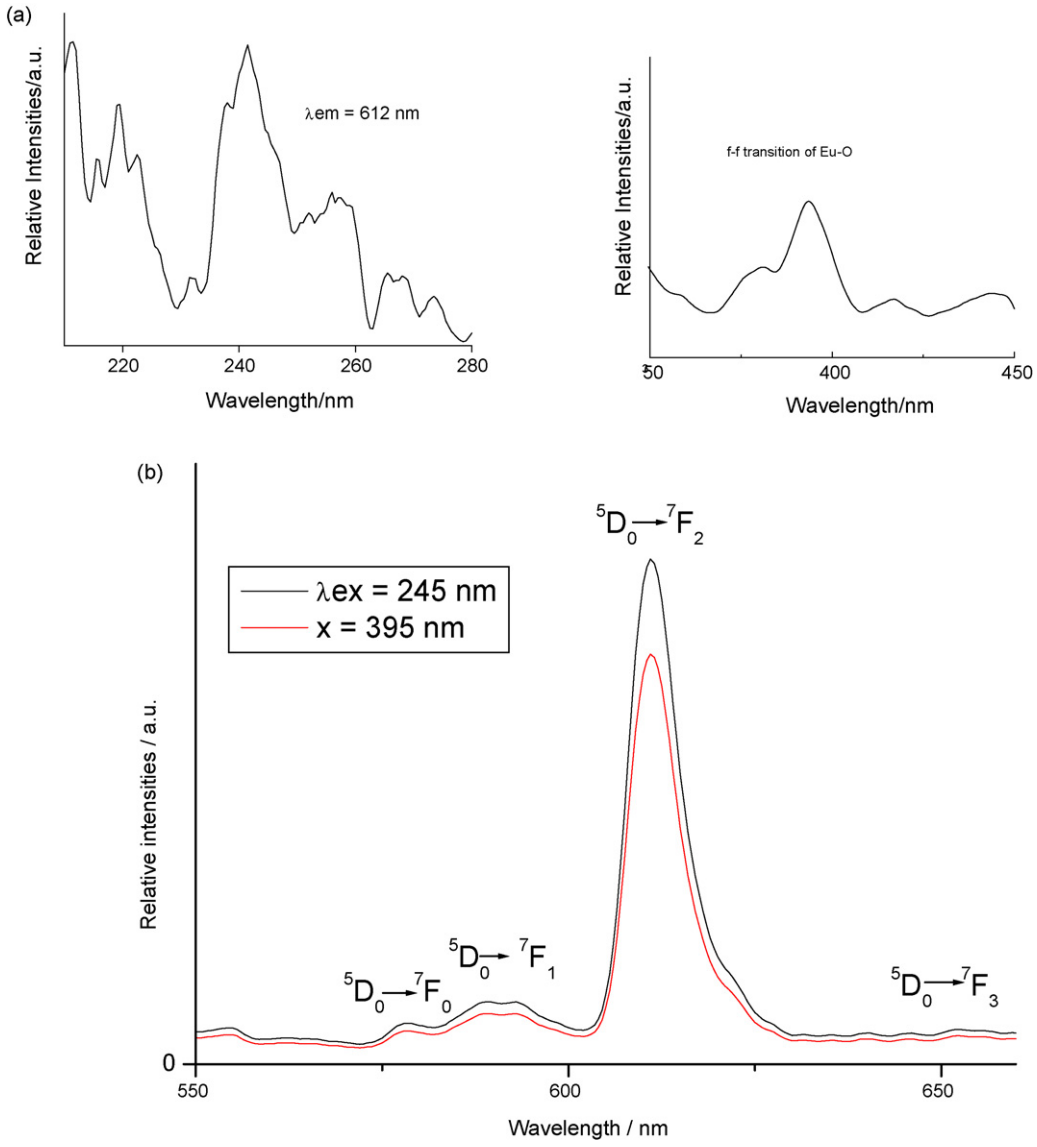

Fig. 7. The excitation (a) and emission (b) spectra of Eu-DBM-MCM-41 hybrids.

Figs. 7 and 8 show the excitation and emission spectra of Eu-DBM-MCM-41 and the Tb-ACAC-MCM-41, respectively. It is noteworthy that the ligand emission background becomes very weak in the two emission spectra, showing that efficient energy transfer from DBM-Si and ACAC-Si to lanthanide ions has occurred. The characteristic emissions of the two covalently bonded hybrid materials with mesoporous host, excited by 242 (or 395) nm for Eu-DBM-MCM-41 and 295 (or 345) nm for Tb-ACAC-MCM-41, show emissions of Eu^{3+} and Tb^{3+} ions. Two narrow emission peaks centered at 592 and 613 nm, assigned to $^5D_0 \rightarrow {}^7F_1$ and $^5D_0 \rightarrow {}^7F_2$ transitions, respectively, were obtained from Eu-DBM-MCM-41. Among the peaks, the emission at 613 nm from the $^5D_0 \rightarrow {}^7F_2$ electronic dipole transition is the strongest, suggesting the chemical environment around Eu(III) ions is in low symmetry without inversion center [45,46]. The emission lines of Tb-ACAC-MCM-41 were assigned to the transitions from the $^5D_4 \rightarrow {}^7F_J$ ($J = 6, 5$) transitions at 490 and 544 nm for terbium ions. Among these emission peaks, the most striking green luminescence ($^5D_4 \rightarrow {}^7F_5$) was observed in the emission spectra which can also indicate that the effective energy transfer took place between the ACAC-Si and the chelated lanthanide ions. Of course, other factors contributing to the green emission still cannot be excluded such as relatively rigid structure of silica gel, which limits the vibration of ligand of Tb^{3+} and prohibits nonradiative transitions. Besides, the different wavelength excitation present the similar emission bands except for the distinction of emission intensity, which suggest that both of the emission are ascribed to the characteristic lanthanide ions energy transfer from the ligands (DBM-Si or ACAC-Si). Accordingly, we may expect that through this efficient way, leaching of the photoactive molecules can be avoided, a higher concentration of metal ions is reached, and clustering of the emitting centers may be prevented.

Furtherly, we compared the luminescent intensities of the hybrid materials and the corresponding complexes according to the Ref. [47]. The concentration of Eu(III) and Tb(III) complexes

Table 2
The luminescence efficiency and lifetimes of the covalently bonded hybrid materials and pure complexes

Systems	Transition	λ_{em} (nm)	τ (ms)	I[a] (a.u.)	C_{Eu} (C_{Tb}) (mol%)	I/C_{Eu} (C_{Tb})[b] (a.u.)
Eu-DBM	$^5D_0 \rightarrow {}^7F_2$	612	0.6954	301	100	3.01
Eu-DBM/MCM-41	$^5D_0 \rightarrow {}^7F_2$	612	0.9085	47	5	9.4
Eu-DBM-MCM-41	$^5D_0 \rightarrow {}^7F_2$	612	1.0735	315	5	63.0
Tb-ACAC	$^5D_4 \rightarrow {}^7F_5$	544	0.5846	325	100	3.25
Tb-ACAC/MCM-41	$^5D_4 \rightarrow {}^7F_5$	544	0.8760	51	5	10.2
Tb-ACAC-MCM-41	$^5D_4 \rightarrow {}^7F_5$	544	1.0265	309	5	61.8

[a] I: emission intensity of transition.
[b] I/C_{Eu} (C_{Tb}): the emission intensity of transition divided by the contents of the Eu or Tb species.

on the MCM-41 support were estimated to 5 mol% [47,48]. The contents of the Eu^{3+} or Tb^{3+} ion in molar percentage [C_{Eu} or C_{Tb} (mol%)] in the complexes (and their hybrid materials) and their relative luminescent intensities (integrated intensities) of the $^5D_0 \rightarrow {}^7F_2$ for Eu^{3+} (or $^5D_4 \rightarrow {}^7F_5$ for Tb^{3+}) are listed in Table 2. It can be clearly seen that the intensity divided by the contents of the Eu^{3+} (or Tb^{3+}) ion) in hybrid materials of MCM-41 are much higher than those in pure complexes, suggesting that in the Eu-DBM or Tb-ACAC complexes, a quenching of the Eu^{3+} or Tb^{3+} luminescence can be induced by the concentration effect and/or the electron–phonon couplings with the third vibrational overtone of the close-lying OH oscillator. Furtherly, the covalently bonded hybrid materials with mesoporous host MCM-41 are also stronger than those of corresponding doped hybrid materials in MCM-41 in spite of the similar molar percentage (mol%), which indicates that the covalent bonding interaction between rare earth β-diketonates and MCM-41 are more suitable for the luminescent of rare earth species and enhance the luminescent intensities than the hybrid materials with weak interaction between them. This special behavior shows that MCM-41 is an effective host for the luminescent species of lanthanide complex for luminescence quenching effect can be decreased in this covalently bonded hybrid materials.

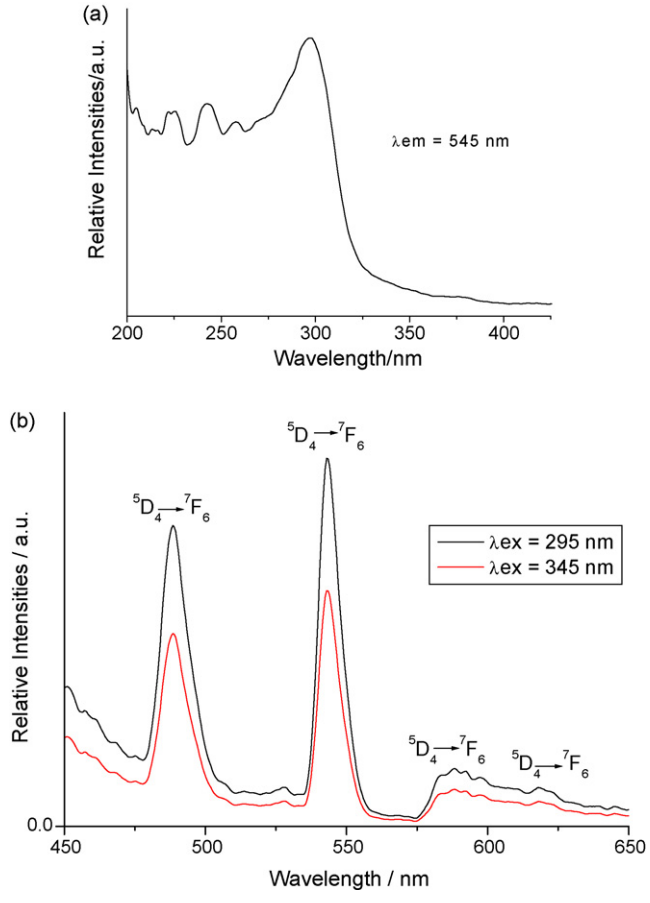

Fig. 8. The excitation (a) and emission (b) spectra of Tb-ACAC-MCM-41 hybrids.

To further investigate the luminescence efficiency and lifetimes of the covalently bonded hybrid materials, we also synthesized Eu-DBM and Tb-ACAC binary complexes, doped hybrid materials (Eu-DBM and Tb-ACAC binary complexes were doped in MCM-41 host) and compared the luminescent properties of them with those of Eu-DBM-MCM-41 and Tb-ACAC-MCM-41. Their time-resolved photoluminescence spectra (figures not shown) were all single exponential, indicating that all the Eu^{3+} and Tb^{3+} ions occupy the same average coordination environment. The respective lifetimes were given in the following Table 2. Maybe there is the H-bonding between the RE complex and the modifying agent, which is connected to the wall of MCM-41. Therefore, much energy is effectively absorbed by the ligands and transferred to the emitting Eu^{3+} and Tb^{3+} ions, and the relaxation time of two hybrid materials covalently bonded MCM-41 in the excited state becomes longer in contrast to pure complexes.

4. Conclusions

In summary, we found that β-diketone ligands (DBM, ACAC) can also be modified as functional bridge molecules (DBM-Si and ACAC-Si) to directly covalently bond mesoporous host (MCM-41). We firstly achieve the modification of DBM, ACAC by a novel chemical path and construct two novel kinds of covalently bonded hybrid materials. The photoluminescent properties indicate that the hybrid materials possess higher luminescent intensities and longer lifetimes, suggesting that covalently boned MCM-41 host can decrease the concentration quenching effect and enhance the luminescent stability. To our knowledge, it is the first example of hybrid materials by modified β-diketone derivatives directly covalently bonded mesoporous host, which can be expected to create a novel technology to apply for these kinds of hybrid materials.

Acknowledgement

This work was supported by the National Natural Science Foundation of China (20671072).

References

[1] J.S. Beck, J.C. Vartuli, W.J. Roth, M.E. Leonowicz, C.T. Kresge, K.D. Schmitt, C.T.W. Chu, D.H. Olson, E.W. Sheppard, S.B. McCullen, J.B. Higgins, J.L. Schlenker, J. Am. Chem. Soc. 114 (1992) 10834.
[2] C.T. Kresge, M.E. Leonowicz, W.J. Roth, J.C. Vartuli, J.S. Beck, Nature 359 (1992) 710.
[3] J. Yu, J.L. Shi, L.Z. Wang, M.L. Ruan, D.S. Yan, Mater. Lett. 48 (2001) 112.
[4] T. Maschmeyer, F. Rey, G. Sankar, J.M. Thomas, Nature 378 (1995) 159.
[5] R. Burch, N. Cruise, D. Gleeson, S.C. Tsang, Chem. Commun. (1996) 951.
[6] M.H. Lim, C.F. Blanford, A. Stein, Chem. Mater. 10 (1998) 467.
[7] S.L. Burkett, S.D. Sims, S. Mann, Chem. Commun. (1996) 1367.
[8] D.J. MacQuarrie, Chem. Commun. (1996) 1961.
[9] C.E. Fowler, S.L. Burkett, S. Mann, Chem. Commun. (1997) 1769.
[10] M.H. Lim, C.F. Blanford, A. Stein, J. Am. Chem. Soc. 119 (1997) 4090.
[11] M. Sasidharan, N.K. Mal, A. Bhaumik, J. Mater. Chem. 17 (2007) 278.
[12] O.C. Gobin, Y. Wan, D.Y. Zhao, F. Kleitz, S. Kaliaguine, J. Phys. Chem. C 111 (2007) 3053.
[13] L. Han, Y. Sakamoto, O. Terasaki, Y.S. Li, S. Che, J. Mater. Chem. 17 (2007) 1216.
[14] C.E. Moran, G.D. Hale, N.J. Halas, Langmuir 17 (2001) 8376.
[15] K.P. Velikov, A. Van Blacacderen, Langmuir 17 (2001) 4779.
[16] A. Moroz, Phys. Rev. B 66 (2002) 115109.
[17] R. Campostrini, G. Carturan, M. Ferrari, M. Montagna, O. Pilla, J. Mater. Res. 7 (1992) 745.
[18] C.X. Du, L. Ma, Y. Xu, W.L. Li, J. Appl. Polym. Sci. 66 (1997) 1405.
[19] D. Chandra, A. Bhaumik, Microporous Mesoporous Mater. 101 (2007) 348.
[20] L. Fernandez, N. Garro, J.M. Morales, P. Burguete, J. Latorre, C. Guillem, A. Beltran, D. Beltran, P. Amoros, Nanotechnology 17 (2006) 4456.
[21] Y. Leydet, F.J. Romero-Salguero, C. Jimenez-Sanchidrian, D.M. Bassani, N.D. McClenaghan, Inorg. Chim. Acta 360 (2007) 987.
[22] K. Dimos, I.B. Koutselas, M.A. Karakassides, J. Phys. Chem. B 110 (2006) 22339.
[23] C. Huo, H.D. Zhang, H.Y. Zhang, H.Y. Zhang, B. Yang, P. Zhang, Y. Wang, Inorg. Chem. 45 (2006) 4735.
[24] Q.G. Meng, P. Boutinaud, H.J. Zhang, R. Mahiou, J. Lumin. 124 (2007) 15.
[25] C. Tiseanu, M.U. Kumke, V.I. Parvulescu, A.S.R. Koti, B.C. Gagea, J.A. Martens, J. Photochem. Photobiol. A Chem. 187 (2007) 299.
[26] C. Sanchez, B. Lebeau, Mater. Res. Soc. Bull. 26 (2001) 377.
[27] A.C. Franville, D. Zambon, R. Mahiou, Chem. Mater. 12 (2000) 428.
[28] H.R. Li, J. Lin, H.J. Zhang, H.C. Li, L.S. Fu, Q.G. Meng, Chem. Commun. (2001) 1212.
[29] Q.M. Wang, B. Yan, J. Mater. Chem. 14 (2004) 2450.
[30] Q.M. Wang, B. Yan, Cryst. Growth Des. 5 (2005) 497.
[31] Q.M. Wang, B. Yan, J. Photochem. Photobiol. A Chem. 175 (2005) 159.
[32] Q.M. Wang, B. Yan, J. Organomet. Chem. 691 (2006) 540.
[33] K. Binnemans, P. Lenaerts, K. Driesen, C. Gorller-Walrand, J. Mater. Chem. 14 (2004) 191.
[34] H.R. Li, J. Lin, L.S. Fu, J.F. Guo, Q.G. Meng, F.Y. Liu, H.J. Zhang, Microporous Mesoporous Mater. 55 (2002) 103.
[35] S. Gago, J.A. Fernandes, J.P. Rainho, R.A.S. Ferreira, M. Pillinger, A.A. Valente, T.M. Santos, L.D. Carlos, P.J.A. Ribeiro-Claro, I.S. Goncalves, Chem. Mater. 17 (2005) 5077.
[36] C.J. Liu, S.G. Li, W.Q. Pang, C.M. Che, Chem. Commun. (1997) 65.
[37] M.C. Goncalves, V. de Zea Bermudez, R.A. Sa Ferreira, L.D. Carlos, D. Ostroviskii, J. Rocha, Chem. Mater. 16 (2004) 2530.
[38] R.B. Laughlin, J.D. Joannopoulos, Phys. Rev. B 16 (1977) 2942.
[39] M.V. Landau, S.P. Parkey, M. Herskowitz, O. Regev, S. Pevzner, T. Sen, Z. Luz, Microporous Mesoporous Mater. 33 (1999) 149.
[40] S. Sato, M. Wada, Bull. Chem. Soc. Jpn. 43 (1970) 1955.
[41] S.L. Wu, Y.L. Wu, Y.S. Yang, J. Alloys Compd. 180 (1994) 399.
[42] D.L. Dexter, J. Chem. Phys. 21 (1953) 836.
[43] T.D. Brown, T.M. Shepherd, J. Chem. Soc. Dalton Trans. (1973) 336.
[44] M. Jaroniec, M. Kruk, A. Saryari, Mesoporous Mol. Sieves 17 (2003) 325.
[45] P. Lenaerts, K. Driesen, R.V. Deun, K. Binnemans, Chem. Mater. 17 (2005) 2148.
[46] L.H. Wang, W. Wang, W.G. Zhang, E.T. Kang, W. Huang, Chem. Mater. 12 (2000) 2212.
[47] Q.H. Xu, W.J. Dong, H.W. Li, L.S. Li, S.H. Feng, R.R. Xu, Solid State Sci. 5 (2003) 777.
[48] C.Y. Peng, H.J. Zhang, J.B. Yu, Q.G. Meng, L.S. Fu, H.R. Li, L.N. Sun, X.M. Guo, J. Phys. Chem. B 109 (2005) 15278.